doi: 10.32131/jes.9.19

Journal of the Earth Simulator, Volume 9, March 2008, 19–26

Internal and External Flow of Rocket Nozzle

Taro Shimizu[1]*, Masatoshi Kodera[2], and Nobuyuki Tsuboi[3]

[1] *JAXA's Engineering Digital Innovation Center, Japan Aerospace Exploration Agency, 3-1-1, Yoshinodai, Sagamihara, Kanagawa 229-8510, Japan*
[2] *Advanced Propulsion Technology Research Group, Space Transportation Propulsion Research and Development Center, Office of Space Flight and Operations, Japan Aerospace Exploration Agency, 1, Koganezawa, Kimigaya, Kakuda, Miyagi 981-1525, Japan*
[3] *Institute of Space and Astronautical Science, Japan Aerospace Exploration Agency, 3-1-1, Yoshinodai, Sagamihara, Kanagawa 229-8510, Japan*

(Received January 5, 2008; Revised manuscript accepted February 13, 2008)

Abstract The objective of this study is to clarify flow structures inside and outside a rocket nozzle, which are indispensable for actual development of rocket engine. One is the transition of the flow structure between free shock separation and restricted shock separation inside a nozzle, which would sometimes generate a destructive side-load. The transition is numerically reproduced under the experimental condition where the transition occurs. We also found a simple function to analyze the flow structure inducing transition. Another is ignition overpressure induced by engine ignition. The overpressure, which originates in shock wave, imposes high pressure load on the nozzle or rocket surface and also influence the ignition process especially under clustering (two) nozzle configuration. The numerical results show that besides an overpressure, a vortex ring is generated and propagated from the nozzle. Under clustering nozzle configuration, the interaction between the overpressure waves and the vortex rings occurs between the nozzles. This makes the force acting on the nozzle asymmetric. We could estimate the side-load acting on the nozzle actuator in advance of the development and firing test.

Keywords: rocket nozzle, RSS, FSS, flow transition, ignition overpressure, RANS

1. Introduction

Understanding the phenomena of the internal and external flow of a rocket nozzle is essential for developing a highly reliable space launch vehicle. Until recently, almost all the development of Japanese rocket elements was based on trial and error, i.e. an iterative cycle of trial design and experimental verification. However, in a new engine development, or an engine improvement for lowering cost and high performance, sometimes latent troubles have included in many components of the rocket, which would unfortunately end in mission failure once in a while. Therefore it is obvious that we need more stores of our own knowledge for the development. Recent progress in computational fluid dynamics has changed the trial and error approach, as numerical simulation is now playing a major role in the development of rockets and rocket engines built today. Fortunately Japan leads the world in supercomputing technology, *e.g.* the Earth Simulator. However, the effective and substantial use of this technology has just begun especially in the industry. In JAXA (Japan Aerospace Exploration Agency), the CFD (Computational Fluid Dynamics) by the supercomputer plays an important role in the development because the CFD results began to provide the reliable answer for development. In other words, the simulation can explain or reproduce the real phenomena. As a result, the role of the simulation is changing; from just a reference of the experiment to the basis of early design process. Since the full-scale experiment of the rocket element is much time and cost consuming, effective use of the CFD will contributes to the development. We think that it gives a hope to complement the luck of experience and limited budget.

In this study, two simulation results are presented, which could contribute to the actual development. One is the verification of the origin of the large side-load at a nozzle, which occurs during the development of the LE-7A engine. Another is on the newly developing H-IIB rocket, which has two liquid engines for the first time in Japan.

* ***Corresponding author***: *Taro Shimizu, JAXA's Engineering Digital Innovation Center, Japan Aerospace Exploration Agency, 3-1-1, Yoshinodai, Sagamihara, Kanagawa 229-8510 Japan. E-mail: shimizu.taro@jaxa.jp*

Estimating the difference of flow fields between single and clustering nozzle configurations is very important issue.

2. Numerical method

A numerical method of solving the Navier-Stokes equations on the hybrid unstructured grid was developed using a finite-volume cell vertex scheme and the LU-SGS implicit time integration algorithm [1, 2]. Figure 1 presents the unstructured grid distribution near the LE-7A original nozzle. The Goldberg -Ramakrishnan model was used to evaluate the turbulent kinetic viscosity, and the Venkatakrishnan limiter function was used to enhance the convergence. In some unsteady calculations, Newtonian sub-iteration was implemented based on the Crank-Nicholson method to ensure time accuracy up to the second order. In order to take the O/F (mixture ratio; mass ratio of oxidizer to fuel) effect into account, the adopted code should treat the properties of gas mixture that consists of multi chemical species. Therefore, the code incorporates the standard finite reaction rate model for the H_2-O_2 reaction including nine species (H_2, O_2, H_2O, H, HO_2, OH, O, H_2O_2, and N_2). The calculation was performed using the Earth Simulator of the Japan Agency for Marine-Earth Science and Technology (JAMSTEC).

3. Transition of the flow structure

Design of a nozzle contour is one of the major factors for an effective rocket engine. Therefore optimization of the nozzle contour has been conducted to obtain maximum thrust under the limits of the whole engine system. So far various kinds of design methods are developed based on classical nozzle design methods, such as conical, parabolic and truncated perfect nozzles, only to increase steady performance [3-5]. However it is also known that such high performance nozzle sometimes causes a large side-load and high thermal stress on the nozzle wall during the transient of the operation. These would induce serious launch problems and also destroy engine hardware in sea-level tests. Therefore the unsteady behavior of the flow structure should be considered in the design process. In order to avoid the destructive side-load, a great deal of work has been done experimentally and numerically to clarify the origin of the side-load generation [6-8]. Inside the thrust optimized and parabolic nozzles, an internal shock is generated by the nozzle contour. This internal shock, usually generated from the throat of the nozzle, forms an inverse Mach reflection at the centerline downstream of the throat, enhancing the momentum of the flow toward the nozzle wall. Therefore, the transition of the flow structure, from FSS (free shock separation) to RSS (restricted shock separation or attached flow) and vise versa, could occur and create the sudden change of the pressure distribution on the nozzle wall, generating the side-load [7, 8].

In developing the LE-7A engine of the Japanese H-IIA launch vehicle, we were faced with a side-load originating in the transition of the flow structure during the start-up and shut-down transients [9-12]. Actually, the nozzle was initially designed as a compressed truncated perfect nozzle (CTP nozzle) which is different from any other nozzles developed. Therefore the study has begun to investigate the origin of this undesired phenomenon. In the start-up and shut-down transient, the O/F is fluctuating sharply in the actual operation. Although the nominal value for the O/F designed for the steady condition is about 6 (hydrogen rich), the transient value can be from 3 to 8 for a short period of time. The subscale experiment [10, 11] demonstrated it is shown that the flow transition from FSS to RSS is likely to occur with a lower O/F than the designed value. Therefore, the start-up transient flow structures for O/F's corresponding to 6 and 3 are investigated in detail. The transition mechanism is explained by analyzing the flow properties that are difficult to obtain by experiment alone.

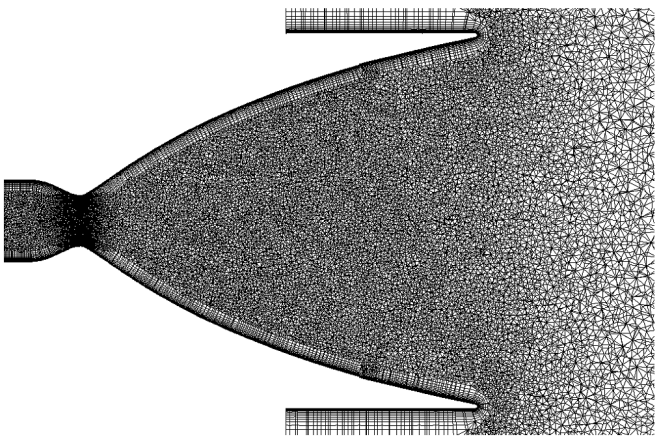

Fig. 1 Unstructured grid distribution on a symmetric plane for LE-7A original nozzle.

Here we briefly explain the numerical settings. The boundary condition of the nozzle inlet is as follows. The reaction of the fuel, H_2 and the oxidizer, O_2, is assumed to be completed upstream of the nozzle inlet (in the combustion camber) under a prescribed mixture ratio. Therefore, H_2O and H_2 flow into the nozzle with a given total temperature and total pressure (only if O/F is less than 8, which corresponds to the stoichiometric ratio). This simplified frozen chemistry model is used mainly for reducing CPU time. However, we conducted preliminary axis-symmetric simulations for non-equilibrium chemistry and found that there was no major difference in the Mach isolines inside the nozzle between the non-equilibrium and the frozen calculation. Therefore, we simplify the inlet condition mentioned above. Initially, inside the nozzle and the surroundings are filled with the standard air (T = 300K, P_a = 0.1MPa). Throughout the calculation, the temperature of the nozzle wall is assumed to be 700K which roughly corresponds to the actual operation.

3.1 Reproduction of the flow transition

Figures 2 and 3 present the snapshot of flow fields showing the FSS and the transition to RSS structure respectively. Here we define the nozzle pressure ratio,

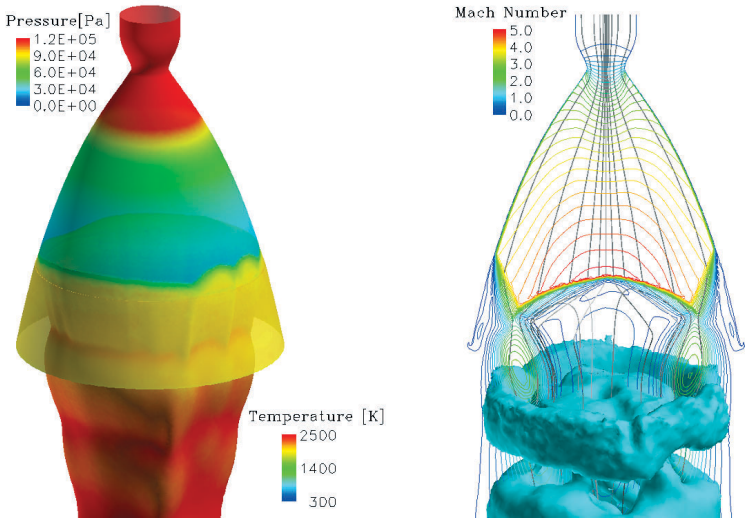

Fig. 2 FSS flow structure. NPR = 52. O/F = 6.
Wall pressure and temperature on the iso-surface where mass fraction of H_2O = 0.6 (left figure). Mach number and large vortical structure (second invariant of velocity gradient tensor) together with stream lines (right figure).

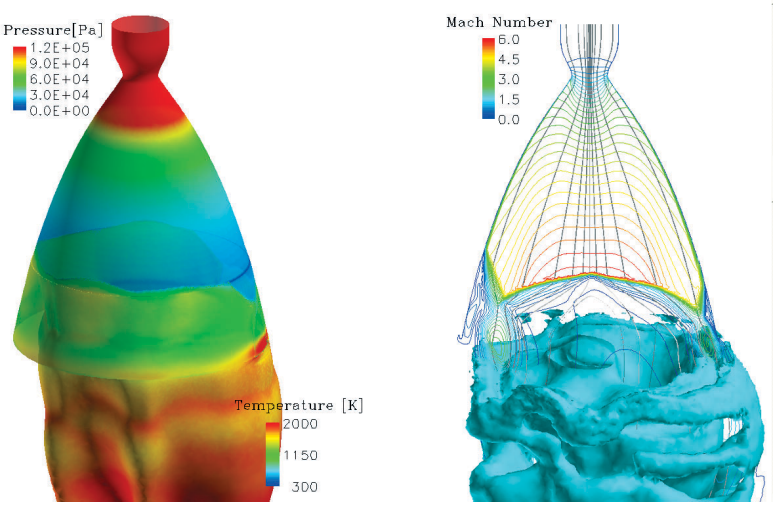

Fig. 3 Transition to RSS flow structure. NPR = 52. O/F = 3.
Wall pressure and temperature on the iso-surface where mass fraction of H_2O = 0.6 (left figure). Mach number and large vortical structure (second invariant of velocity gradient tensor) together with stream lines (right figure).

NPR = P_c / P_a, where P_c is the chamber pressure. The rate of the pressure increment is set about 0.05 [NPR / msec], which is of the same order as in real operation of this range. When O/F = 6 (Fig. 2), the separation line remains nearly symmetric (throughout all transient state). The wall pressure behind the separation line remains at ambient pressure. This means the hot combustion gas is apart from the nozzle wall. Mach isolines also indicate the flow has FSS structure. The vortical structure represents that the downstream of the nozzle exit, there generates series of stable symmetrical vortex rings as NPR increases. When O/F=3 (Fig. 3), the region between the supersonic jet and the wall narrows. In this region, aspired inflow of ambient air is accelerated, resulting in decreased wall pressure (the green part of the nozzle wall pressure upstream of the nozzle exit). Since the separation shock location is determined to balance the pressure gap, once the wall pressure downstream is decreased, the corresponding part of the separation line moves downstream inducing a further decrease in wall pressure. Thus, part of the deformed separation line moves downstream suddenly, generating the recirculation bubble and RSS flow structure shown in right part of the nozzle wall (observed as in wall pressure and Mach isolines). The imbalance of the circumferential pressure distribution (the different flow structure between FSS and RSS) generates a large side-load. The vortical structure downstream of the nozzle exit becomes asymmetric indicating that the flow is unsteady and unstable. A comparison of the magnitude of side loads between calculated and measured is conducted. The magnitude of the calculated side-load is 120 kN when O/F = 3, which is in accord with the firing test (75~100 kN). Although a slight distortion of the separation line is observed when O/F = 6, the supersonic jet stays away from the nozzle wall (Fig. 2). Therefore, the magnitude of the calculated side-load is 20 kN. The agreement between the simulation and the experiment in the NPR where the large side-load occurs and the O/F at which the transition from FSS to RSS is obtained is reasonably good (NPR = 35~59 and O/F = 2.8~4.1 in the subscale experiment) [10]. Therefore it is shown both in CFD and experiment that the O/F, in other words, the ratio of specific heat has an essential effect on the flow transition.

3.2 Detection of the fine flow structure

Next, we investigate the obtained flow structure in detail to find some design standard. This is particularly important for the actual development process where the large simulations conducted here are not usually applicable. It is known that inside thrust optimized and parabolic nozzles, an internal shock is generated from the throat and an inverse Mach reflection at the centerline downstream of the throat forms a cap shock structure. Thus, the momentum of the flow toward the nozzle wall increases, hence pushing the supersonic jet toward the nozzle wall resulting in the generation of RSS flow. However, little is known about a CTP nozzle studied here. In particular, although the cap shock structure is observed independent of the O/F, it is not clear whether the bending contour of the Mach number corresponds to the existence of an internal shock wave, which is characteristic of thrust optimized and parabolic nozzles. Therefore, using the shock function [13], we first investigate whether an internal shock exists. The shock function is defined as follows:

$$f(\mathbf{x}) \equiv \frac{\mathbf{u}}{\mathrm{c}} \cdot \frac{grad\,\mathrm{p}}{|grad\,\mathrm{p}|},$$

where **u** is the velocity, c is the acoustic speed and p is the pressure. This function represents the Mach number ($\mathbf{u}/c$) of the velocity component perpendicular to the pressure discontinuity. Therefore, if a shock wave exists, the function changes from greater than 1 upstream to less than 1 downstream. We applied this function to the obtained flow field. However, no shock wave is detected around the bending Mach contour inside nozzle. Compression waves generated from the wall contour downstream of the initial expansion (circular arc) may coalesce into a shock wave depending on the compression ratio of the truncated perfect nozzle. We believe that for the CTP nozzle studied here, the internal shock wave, if existed, is too weak to be detected by the shock function under the mesh size used. Therefore it is necessary to investigate in detail the compression and expansion in the flow fields for understanding the difference of flow structures with varying O/F. Here, we introduce the compression function defined below [14]:

$$C(\mathbf{x}) \equiv \frac{grad\,\mathrm{p}}{\mathrm{p_c}} \cdot \frac{\mathbf{u}}{|\mathbf{u}|}.$$

This function becomes positive (negative) when the pressure increases (decreases) along a stream line. Note that this function has a dimension (1/m). Figure 4 shows the compression function applied for steady full flow condition (NPR = 124). The blue part indicates the expansion region where the flow is efficiently expanded by the nozzle. The red part including the shock wave which can be detected by the shock function, indicates the region where the flow is not expanded or accelerated efficiently. A strong correlation is observed between this low-expansion region and the contour of the Mach number. The concentrated and bending contour corresponds closely to the low-expansion region (thin triangular red region). By this

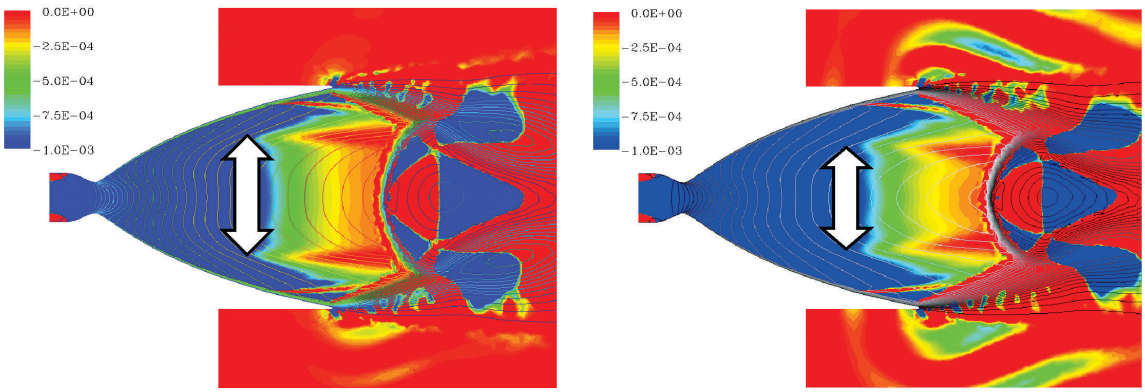

Fig. 4 Compression function [1/m] and Mach number distribution (contours), O/F = 3 (left figure). O/F = 6 (right figure).

low-expansion region, we can roughly know the internal core, where the contour of the Mach number becomes nearly perpendicular to the nozzle axis, and the outer region bounded by the separation shock from the nozzle wall. When O/F = 3, the internal core becomes broad radially. Therefore, the curvature of the Mach isolines is small. This results in a small curvature of the cap shock downstream. It is quite natural that the curvatures are similar because the shock wave is formed to balance the flows passing through the shock wave itself. Another notable point is that the radial widths of the outer boundary of the low-expansion region and the end of the cap shock downstream are nearly identical. Since there is no precise theory to describe the Mach reflection or the oblique shock in an axis-symmetric flow configuration, it is very difficult to analytically explain the flow structure inside a nozzle. However, it is worth noting that the compression function applied here reveals a strong correlation between the outer boundary radial widths of the low-expansion region and the end of the cap shock. This function captures the mild compression flow structure inside the nozzle where an internal shock is not detected and helps to understand the flow transition between FSS and RSS without conducting unsteady simulation.

The present nozzle design for LE-7A engine is classical truncated perfect nozzle which is considered to be the most robust nozzle design, but not to have highest performance. Therefore there is room for developing a high performance nozzle without undesired unsteady phenomena in the future.

4. Generation of the overpressure in the start-up transient of the rocket engine

The H-IIB launch vehicle, which is an upgraded version of the current H-IIA launch capacity, is under development (Fig. 5). The H-IIB launch vehicle has two major purposes. One is to launch the H-II Transfer Vehicle (HTV) to the International Space Station (ISS). The other is to respond to broader launch needs by making combined use of both H-IIA and H-IIB launch vehicles. To obtain larger launch capability, the H-IIB has clustering (two) liquid rocket

Fig. 5 Schematic of newly developing H-IIB launch vehicle. The clustered LE-7A are installed as the first stage engine.

engines (LE-7A) in the first-stage, instead of one for the H-IIA. The efficient development is expected based on the use of the knowledge obtained so far.

Since this is for the first time in Japanese rocket having two liquid rocket engines clustered, the estimation of the difference of flow fields between single and clustering nozzle configurations is very important. In this study, the generation of the large pressure disturbance at the start-up transient, called ignition overpressure is numerically investigated in detail, which is one of the concerns on the modifications. The ignition overpressure is originally well recognized in solid rocket booster [15-17]. However, since the two liquid engines are designed to be located very close, the mutual influence of pressure disturbances and flow structure around nozzles should be investigated in detail.

First, the flow under original single nozzle configuration is simulated for verification (not shown here). The numerical method is the same as the previous section except that the mass fractions of the each species are obtained from the chemical equilibrium calculation. The transient operation is modeled as follows. The total pressure is linearly increased from the atmospheric pressure to the first peak of the chamber pressure (2.6MPa), where the influence of the overpressure is almost disappeared. The total temperature is set 3560K throughout the calculation which corresponds to the chemical equilibrium state of the chamber. The rate of the pressure increase is set about 1 [NPR/msec] which is the same as the actual operation. The result shows that at the start-up transient, an overpressure and a vortex ring are generated and propagated downstream from the nozzle. As the NPR increases, the overpressure arrives at the nozzle tip decreasing its amplitude, and then propagates nearly spherically from the nozzle. At the same time, vortex ring is made by the shear and impulse, which propagates downstream of the nozzle. The tip wall pressure is compared with the experiment for verification of the simulation. The positive pressure disturbance (from the atmospheric pressure) is observed first, which corresponds to the overpressure, and then the negative pressure disturbance is observed, which corresponds that the vortex core is generating, dissipating and moves downstream. The peak amplitude and the time lag between the overpressure and the vortex ring are in good agreement between CFD and experiment.

Based on this preliminary study, we estimate that when the nozzles are clustered, the pressure disturbance induced by the neighboring nozzle is 10% of the atmospheric pressure. Therefore, the influence of the disturbance is not enough to deform the separation line which induces the side-load. However, under the clustering nozzle configuration, the interaction between the overpressure waves and the vortex rings may occur especially between the nozzles. Therefore we next investigate the transient flow structure with clustered nozzle configuration.

Figure 6 shows time series of the numerical result for the simultaneous start-up. All colored contours and surfaces represent the pressure field; pressure of nozzle outside wall, iso-surface (9.0E+4 and 1.09E+5 Pascal) of the pressure and the slice of the pressure on the symmetric surface are shown. The contour for Mach number is also plotted as observed inside the nozzle. As NPR increases, the overpressure propagates outside the nozzle nearly spherically and interacts between nozzles (Fig. 6a). The weak pressure disturbance (as seen by small circle in Fig. 6a.) is the weak sound propagating from the wall which has initially different temperature form the ambient. It is verified that the influence is negligible by the calculation of adiabatic wall. We can also observe the generation of the vortex rings by green tori. When NPR = 9 (Fig. 6b), the interaction of the overpressure stands out and generates the positive pressure disturbances on the inner side of nozzle walls, which generates repulsive force between nozzles. Then it is found that the interaction of two vortex ring (shown as merging green tori in pressure field of Fig. 6c-d) occurs, which induces the anomalous behavior that the inner part of the interacting vortex ring propagates upstream. This irregular behavior can be understood by the motion of the two dimensional vortex pair whose magnitude of the vorticity is the same but has opposite sign. As a result, it generates negative pressure disturbances and asymmetric wall pressure distribution on each nozzle. Thus, the force acting on the nozzle becomes attractive force between nozzles this time.

Based on the result obtained, we estimate the side-load acting on the actuator of the nozzle, which is necessary for the development. Due to the symmetry of the configuration, the forces acting on the four actuators of two nozzles behave nearly the same for repulsive and attractive force mentioned above. Figure 7 shows the normalized loads acting on the four actuators of the nozzles. The negative and positive loads correspond to the repulsive and attractive force between nozzles respectively and have nearly the same amplitude. The positive load has larger time scale than the negative load, because of the slow propagating velocity for the vortex rings. It is also observed that the positive loads obtain high frequency disturbances, which originates in the jet noise generation. The peak and the frequency of the loads (about 50 Hz) are expected by this numerical result, which is taken into consideration at the early development process before the firing test.

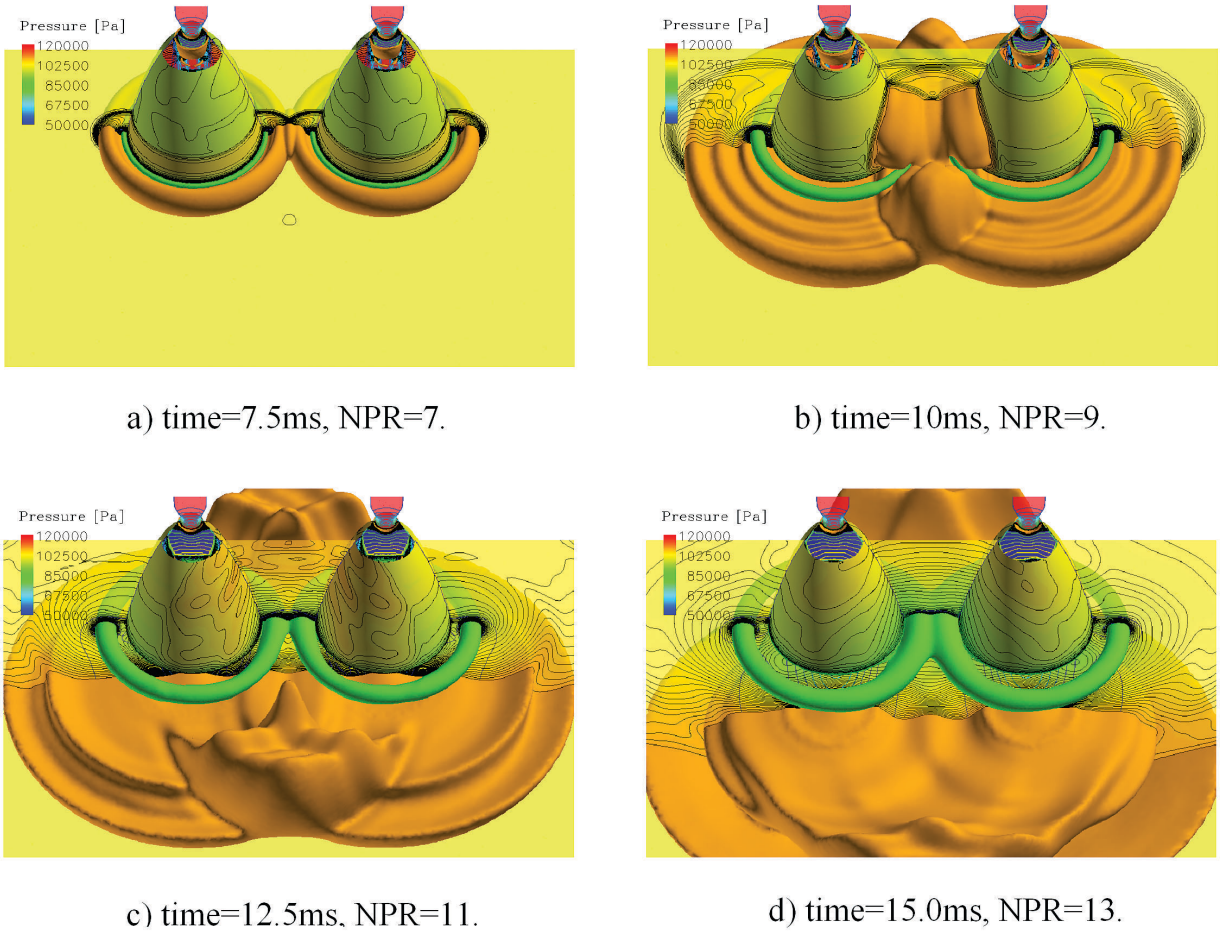

Fig. 6 Time series of the pressure and Mach number distributions for simultaneous start-up of H-IIB rocket.

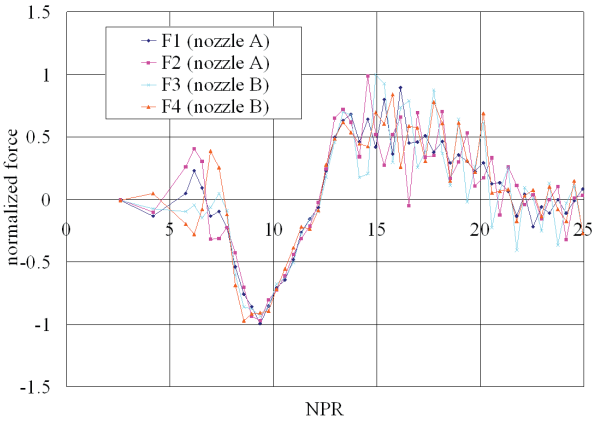

Fig. 7 Normalized loads acting on the four actuators of the nozzles.

5. Conclusions

Two simulation results were presented, that could contribute to the actual development of the rocket engines. One is the verification of the origin of the large side-load at a nozzle we have faced during the development of the LE-7A engine. The transition of the flow structure from FSS to RSS inside a nozzle was numerically reproduced and explained. The mixture ratio is the key to determining flow structure. A simple method using the compression function is proposed to capture the flow structure and understand the transition. Another is on the newly developing H-IIB rocket which has two LE-7A engines. The estimation of the difference of flow fields between single and clustering nozzle configurations is very important issue. In this study, the generation of the large pressure disturbance at the start-up transient by the interaction between ignition overpressures and vortex rings were investigated in detail. The peak and the frequency of the loads were estimated by the numerical results, which is taken into consideration at the early development process before the firing test.

(This article is reviewed by Dr. Tetsuya Sato.)

References

[1] M. Kodera, T. Sunami, and K. Nakahashi, Numerical Analysis of SCRAMJET Combusting Flows by Unstructured Hybrid Grid Method, *AIAA Paper*, 00–0886,

2000.

[2] Tohoku University Aerodynamic Simulation Code (TAS).

[3] M. J. Zucrow and J. D. Hoffman, *Gas Dynamics*, vol.**2**, John Wiley and Sons, New York, pp.160–164, 1977.

[4] G. V. R. Rao, Exhaust Nozzle Contour for Optimum Thrust, Jet Propulsion, vol.**28**, pp.377–382, 1958.

[5] J. D. Hoffman, Design of Compressed Truncated Perfect Nozzles, *Jet Propulsion*, vol.**3**, no.2, pp.150–156, 1987.

[6] L. H. Nave and G. A. Coffey, Sea Level Side Loads in High-Area-Ratio Rocket Engines, *AIAA Paper*, 73–1284, 1973.

[7] M. Frey and G. Hagemann, Restricted Shock Separation in Rocket Nozzles, *Journal of Propulsion and Power*, vol.**16**, no.3, pp.478–484, 2000.

[8] G. Hagemann, M. Frey, and W. Koschel, Appearance of Restricted Shock Separation in Rocket Nozzles, *Journal of Propulsion and Power*, vol.**18**, no.3, pp.577–584, 2002.

[9] Y. Watanabe and M. Tsuboi, LE-7A Engine Nozzle Problems during Transient Operations, *AIAA Paper*, 02–3841, 2002.

[10] T. Tomita, H. Sakamoto, M. Takahashi, M. Sasaki, T. Tamura, and M. Tsuboi, Sub-Scale Nozzle Combustion Tests of the LE-7A Engine for Clarification of Large Side-loads(I): Formation of RSS Structure Due to Combustion Condition, *AIAA Paper*, 02–3842, 2002.

[11] T. Tomita, H. Sakamoto, T. Onodera, M. Sasaki, M. Takahashi, H. Tamura, and Y. Watanabe, Experimental Evaluation of Side-load Characteristics on TP, CTP and TO nozzles, *AIAA Paper*, 04–3678, 2004.

[12] M. Takahashi, S. Ueda, T. Tomita, M. Takahashi, H. Tamura, and K. Aoki, Transient Flow Simulation of a Compressed Truncated Perfect Nozzle, *AIAA Paper*, 01–3681, 2001.

[13] D. Lovely and R. Haimes, Shock Detection from Computational Fluid Dynamics Results, *AIAA Paper*, 99–3285, 1999.

[14] T. Shimizu, H. Miyajima, and M. Kodera, Numerical Study of Restricted Shock Separation in a Compressed Truncated Perfect Nozzle, *AIAA Journal*, vol.**44**, no.3, pp.576–584, 2006.

[15] H. Ikawa and F. S. Laspesa, Ignition/Duct Overpressure Induced by Space Shuttle Solid Rocket Motor Ignition, *Journal of Spacecraft*, vol.**22**, no.4, pp.481–488, 1985.

[16] D. L. Pavish and J. E. Deese, CFD Analysis of Unsteady Ignition Overpressure Effect on Delta II and Delta III Launch Vehicles, *AIAA Paper*, 2000–3922, 2000.

[17] F. Canabal and A. Frendi, Study of the Ignition Overpressure Suppression Technique by Water Addition, *Journal of Spacecraft and Rockets*, vol.**43**, no.4, pp.853–865, 2006.